Prediction of Weld Penetration in Circular Laser Welds of Ferritic Steel (P91) Material

Y. V. Harinath[1], K. A. Gopal[2], S. Murugan[2], S. K. Albert[3]
[1] Water & Steam Chemistry Division, Chemistry Group, Bhabha Atomic Research Centre, Kalpakkam
[2] IDEAS, [3] Materials Technology Division, Metallurgy & Materials Group,
Indira Gandhi Centre for Atomic Research, Kalpakkam

ABSTRACT

Any weld designer will always try to design a weld joint with as much low heat input as possible, at the same time obtain a good depth of penetration and in the process maintain minimum heat affected zone. When a tube or a rod has to be welded using a process and if a design analysis can be done, prior to freezing of the design, to find the depth of penetration, then it may raise the confidence level of the weld design. By this way we can avoid wasting time in carrying out random trials. In the present work an approximate method of predicting the depth of penetration during welding over the peripheral of a circular rod has been formulated under Laser Welding Process. This method will be helpful to design the joint with enhanced efficiency and with lesser probability of defects like lack of penetration and excess penetration. In the analysis 'Thermal Explosion" theory has been used to predict the depth of penetration to map the fusion zone of a circular weld joint on P91 rod. The calculated depth of penetration has been compared with the measured depth of penetration on the weld carried out on a rod using Laser Welding process and the results were found to be nearly matching. It has been found that the depth of penetration increases as the welding progresses over the rod and the difference between the depth of penetration between starting & ending points is around a few microns. This is due to the buildup of heat in the cross section of the rod as the weld progresses.

1.0 INTRODUCTION

Modified type 316 austenitic stainless steel namely alloy D9 is currently used as material for clad tube of fuel pins in Indian Prototype Fast Breeder Reactor, which is designed for mixed oxide of Pu & U as the fuel. To achieve high burnup it is proposed to use metallic fuel in lieu of oxide fuel in future and the clad material being considered for this is ferritic steel because of its better swelling resistance than the austenitic stainless steel under the high neutron flux that prevail in the Fast Breeder Reactors [1]. Hence P91 a ferritic steel with 9 wt.% Cr and 1 wt.% Mo, is being considered as a candidate material for the clad tube of fuel pin of future cores of Fast Breeder Reactors. One of the steps involved in the production of fuel pins is the welding of the clad tube to end plug. Gas Tungsten Arc [2] and Laser Beam [3] Welding are the two processes that are currently being used for end plug welding of fuel pins made of austenitic stainless steels. These processes are also being considered for welding of fuel pins with ferritic steel as cladding material. The fuel clad tubes are of 6.6 mm outer diameter with 0.45 mm wall thickness. Hence work is being done to develop a suitable procedure for welding P91 steel end plug with P91 steel clad tube using Laser Beam Welding process [4]. As a part of the above development work, an analysis work has been done to estimate the depth of penetration during circumferential welding of P91 clad tube with P91 end plug using Laser Beam Welding. This procedure has already been employed for predicting the depth of penetration in GTAW process on austenitic stainless steel rods of similar dimensions [5].

2.0 THEORETICAL WORK

2.1 Thermal Explosion Theory:

'Thermal Explosion' is said to occur when a specific quantity of heat is suddenly released into an infinitely extended body [6]. The source of heat could be a sudden chemical reaction, nuclear reaction or electrical short circuiting. Here, we assume that the area of heat source is very negligible and hence it is considered as point heat source. It is also assumed that the material receiving the heat is infinitely extended, homogeneous and isotropic. It follows that the quantity of heat added will transform in the form of increase in enthalpy of the surroundings due to the diffusion of heat. Increase in temperature 'T' at any point having a distance 'r' from the point of heat addition at an instant 't' seconds from the time of heat addition is given by [6]:

$$T_{(r,t)} = \frac{Ho}{(4\pi at)^{1.5}\ \rho\ C_p} \exp\left(\frac{-r^2}{4at}\right) \quad (1)$$

Where,

H_o = Quantity of heat added in KJ

a = Thermal diffusivity of material in m^2/s

p = Density of material in Kg/m^3

C_p= Specific Heat Capacity of the material in KJ/Kg K

2.2 Methodology of Analytical Calculation:

In this work an attempt has been made to predict the depth of penetration during the circumferential welding of P91 tube with P91 end plug and to map the fusion zone in the welded cross section and to compare with the depth of penetration in the actual weld sample. Following assumptions have been made during the analysis:

1. Heat source is a pointed one and occupies negligible area.
2. Heat is added instantaneously to the body.
3. Equation (1) is applicable to the body that extends infinitely in all the directions. However the equation has been applied to a finite size medium in the present work.
4. Latent heat of fusion has not been taken into account.
5. Material properties of the base material changes with change in temperature, but in this calculation these properties have been taken at a specific temperature (200°C).
6. Loss of heat to the surroundings through radiation and convection has not been considered.

For our study we have considered rods of P91 material having a diameter 6.6 mm. This rod geometrically approximates the P91 clad tube with P91 end plug. Welding over the circumference of the rod is considered at a cross section through 360°. The heat of focused laser beam falls on a negligibly small area on the curved surface of the rod. The cross section of the rod can be divided into 36 parts, that is, each part will be a 10 degree sector of the circular cross section. Hence we have 36 nodes. As the heat source is continuously moving, it is assumed that the heat is added instantaneously at the nodes in a sequential manner after a specified time interval. The total time taken to weld the joint can be calculated from the speed of welding. This time duration divided by the number of nodes will give the average time of application of instantaneous heat between the two adjacent nodes t_{node}.

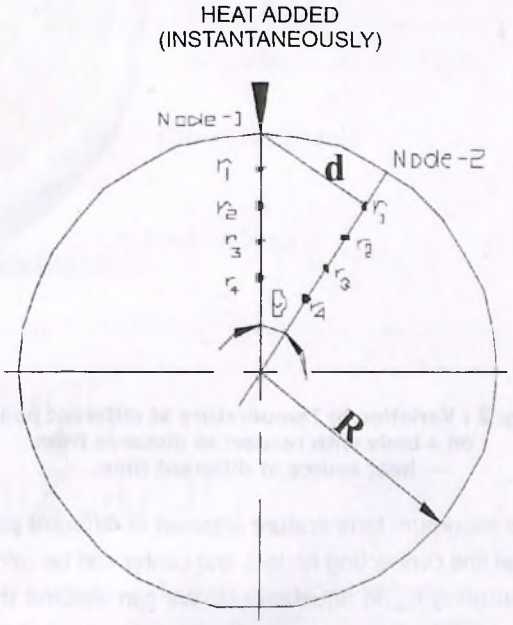

Fig. 1 : Points on line joining the node and center of the rod

The distance, 'd', as shown in the **Fig.1**, is between the node at which heat is added and the point at which the temperature is calculated (r_1, r_2, r_3,.....) can be calculated using the equation-2 given below,

$$d = R^2 + (R-r)^2 - 2\ R\ (R-r)\ \text{Cos}\ \theta \quad (2)$$

Where,

R = radius of the rod

r = radius (distance from point of measurement to center of rod)

θ = angle subtended by two consecutive nodes at the center

Let us assume that the rod is initially at room temperature. Now consider that the heat is added at node-1 instantaneously.

The heat will diffuse into the rod in all direction from node-1. Let us take various points that are at equidistance, along the radius connecting the center and node. The maximum temperature attained at any point reduces as the distance from the point of application of heat source (nodal point) to that point increases. Also the temperature at any point increases initially, attains a peak and then decreases with the progress time. At any point the maximum temperature attained will be at a specific instant, say t_{max}. This is indicated in **Fig. 2** and progression of heat in the rod with instantaneous addition of heat at one point is given in **Fig. 3**. This t_{max} is obtained from the general solution of the equation (1) and is given by:

$$t_{max} = \left(\frac{r^2}{6a} \right) \qquad (3)$$

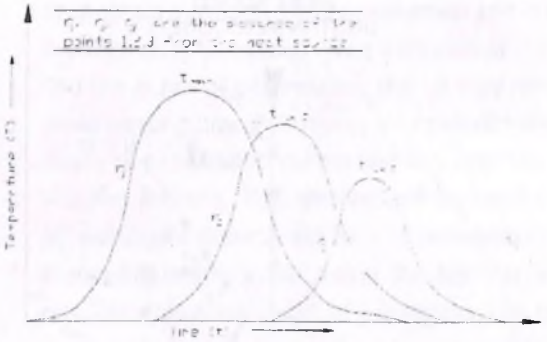

Fig. 2 : Variation in Temperature at different points on a body with respect to distance from heat source at different time.

Now the maximum temperature attained at different points in the radial line connecting node-1 and center can be calculated by substituting t_{max} in equation (1). We can assume that the points at which the temperature has exceeds 1475°C, the melting of the rod has taken place. When the heat source shifts to node-2, the temperature is calculated along the radial line connecting node-2 and center taking the effect of heat addition at node-2 & node-1 by considering the appropriate distances & time durations. It can be noted that due to the addition of heat at node-1, the temperatures at the points on the radial line with node-2 will be initially more than room temperature. This temperature rise due to the heat addition at node-1 is calculated using the equation (1) by taking the time equal to $(t_{node} + t_{max})$ and the appropriate distance. The final temperature at any point on the radial line connecting node-2 and center is now the sum of initial room temperature, increase in temperature due to addition of heat at node-1 and the temperature rise due to the heat addition at node-2. Similarly when the heat source moves to node-3, the final temperature

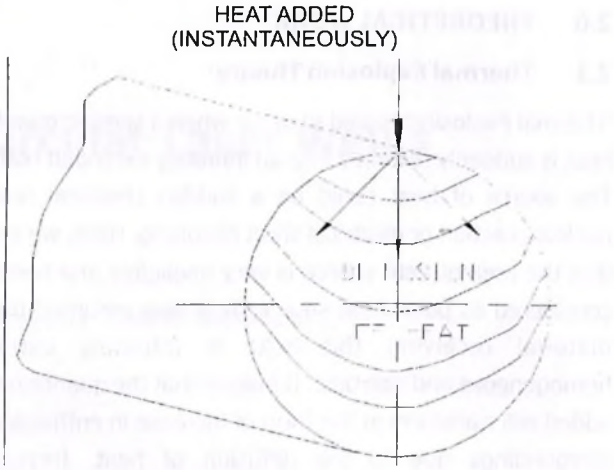

Fig. 3 : Progression of Heat when added to a circular road (Thermal Explosion)

at any point on the radial line connecting node-3 and center will be the sum of initial room temperature, increase in temperature due to addition of heat at node-1, increase in temperature due to addition of heat at node-2 and the temperature rise due to the heat addition at node-3. In this way the temperatures are calculated at different points along the radial lines and the depth of molten region at each node is marked. By plotting the penetration points of all the nodes we can map the fusion zone of a weld bead at a cross section of a rod. In our calculation it was found that the temperature raise beyond 10th node due to the addition of heat at 1st node was less than 3°C. Hence the effect of temperature rise at a node due to the heat added at more than 10 nodes (>90 degree ahead of the node), preceding the node in consideration, is neglected.

It can to be noted that the equation used has been derived for heat addition to an infinite body in which the heat can diffuse in all directions. But in our study the heat is added to a finite body, which is a circular rod and hence it is expected that the predicted penetration could vary from the actual penetration.

This analysis was carried out for rods of three different diameters (5.5mm, 6.6 mm & 8 mm) and welding parameters employed are given in **Table 1** and material properties considered are given below.

Thermo-physical properties of P91 material [7]:

Radius of the rod	= 3.3 mm
Thermal Diffusivity (a) (@200°C)	= 7×10^{-6} m^2/s
Density (p) (@200°C)	= 7680 Kg/m^3
Specific Heat Capacity C_p (@200°C)	= 0.523 KJ/Kg K

Using the above data, detailed calculations were carried out in Microsoft Excel for the weld penetration in 5.5 mm, 6.6 mm & 8

Sigma Weld™
Digital Welding Inverters for MMA, TIG, MIG

Features You Can Think Of We Can Make It Happen.

X-Ray Quality Weld

Energy Efficient

Portable & User Friendly

Safety & Reliability

Robust & Versatile

100% Made in India

Our Product, Your Customization

Choose According To Your Requirements

Sigma Weld is completely designed and developed at our R & D center in Mumbai, India. We have a strong R & D team to meet any specific requirements of our customer. Our technical support team is well trained and equipped to ensure service within 24 hrs anywhere across India

SigmaWeld Welding Inverter's 170 To 1000 ampere

Design Elements

Electronics Devices
Making things happen

Sigma Therm

31, Mistry Industrial Complex,
Cross Road 'A', M.I.D.C,
Andheri (E), Mumbai 400093.
INDIA.

Sigma CapSeal

Sales-T: +91.22.26874629
Service-T: +91.22.26870649
F: +91.22.26870443

Sigma Weld

E: sigmaweld@edmail.in
W: www.electronicsdevices.com
www.sigmaweld.com

© INDIAN REGISTER OF SHIPPING 1993

MGMT. SYS. RvA C 071

WELDING LEGENDS for 35 YEARS An ISO 9001 CERTIFIED COMPANY

memco®

Synonymous with welding

The Only Answer to any "Complex" Welding Applications

Our presence is there in almost all core industries in India & Abroad

Precision Welding Achieves Greater Yield At Low Cost

MPT Memco Power & Tools

MIWT Memco Institute of Welding Training

TCC Tameer Construction Company

RENTNWELD (MEW)

memco guarantees 100% radiographic weld with any specification/ classification of consumable

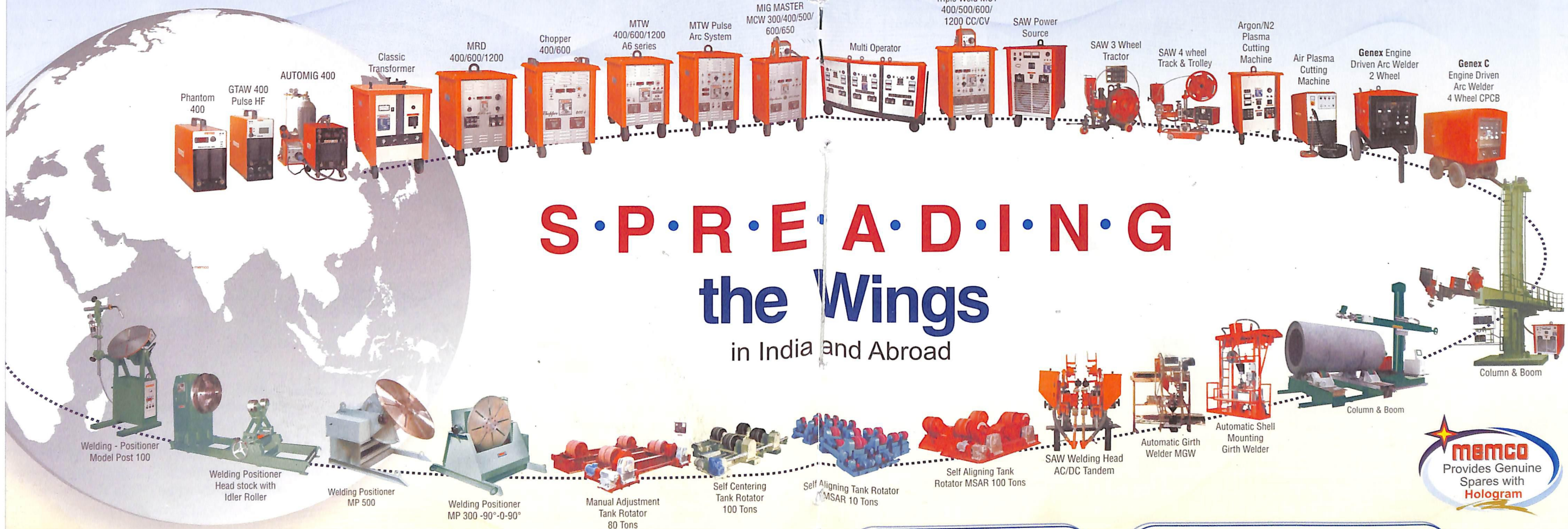

S·P·R·E·A·D·I·N·G the Wings

in India and Abroad

- Totally focused manufacturers of Cutting and welding equipments in SMAW, GMAW, FCAW, GTAW, SAW, Plasma Cutting with Welding Accessories Custom- built equipments and Welding Automation Systems.
- Available with Energy Saver for No Load-Zero Amp.,Power consumption and Safe Welding Device (VRD)
- Also manufacturing World Class range of Welding Tank Rotators from 10kg - 800 tons capacity and all sizes of Column Boom, Welding Positioner etc.,

memco Provides Genuine Spares with Hologram

Electrode Drying Ovens

Power & Tools

Miraj Electrical & Mechanical Co. Pvt. Ltd.

Swastik Chambers, Chembur, Mumbai 400 071, INDIA • Tel. (022) 6797 8091/92/93, 2522 2818/ 2702 • Fax: 91-22-2522 6661

E-mail: memcosales@memcoin.com • memco3@vsnl.com • Service: memcocare@memcoin.com Website: www.memcoin.com

IIW/581-2012

GEE Limited is now India's sole agent for
Mitsubishi Cobalt Alloys.

MITSUBISHI
A MITSUBISHI MATERIALS CORPORATION

Mitsubishi - the world's No.1 brand for Cobalt Alloys is now in the market with its association with GEE Limited - the leaders in welding solutions and the owners of the prestigious 'GWeld' brand. Cobalt Alloys are widely used in Automobile, Steel & Metal processing, Wood pulping, Petrochemical and various other industries. GEE Limited with its proven track record and decades of experience in serving you the best quality products, will now be India's sole agent for Cobalt Alloys from Mitsubishi.

The product is available in 3 forms: Bare Cast Rod, Electrode Transferred Arc Powder & Plasma Transferred Arch Powder (PTA powder) available in grades - Grade-1, Grade-6, Grade-12 and Grade-21.

For further information and assistance please contact us at
bikashmohanty@geelimited.com / uagarwal@geelimited.com or
Call +91 22 25821277.

Registered Office & Thane Plant: Plot No.E-1, Road No.7, Wagle Indl. Estate, Thane-400 604, Maharashtra, India Tel: 91-22-25821277, Fax: 91-22-25828938

Kalyan Plant: Plot No.B-12, MIDC, Kalyan Bhiwandi Road, Saravali, Kalyan-421 311, Thane, Maharashtra, India. Tel: 91-2522-280358/281176/88/90, Fax: 522-281199.

Table 1 : Laser Welding Parameters:

Peak Power (PP)	1.3 KW		
Average Power of heat source	0.157 KW		
Pulses frequency	20 Hz		
Pulse duration (D)	6 ms		
Welding Speed	140 mm/min		
Number of nodes considered	36		
Diameter of rods (mm)	5.5	6.6	8
Time taken for the weld (sec)	7.4	8.88	10.77
Total Heat Energy Imparted (J)	1162	1394	1691
Average heat added per node (J) (H_o)	32.3	38.7	47.0
Time between two subsequent heat additions at adjacent nodes (sec)	0.2056	0.2467	0.2992

Table-2 : Temperatures (°C) attained in different depths at various nodes in 5.5 mm diameter rod

	Final Temperature (°C) attained									
Radial Distance (r) (in mm)	T_{n} at node-I	T_{o} at node-2	T_{o} at node-3	T_{u} at node-4	T_{n} at node-5	T_{n} at node-6	T_{n} at node-7	T_{n} at node-8	T_{n} at node-9	T_{no} to T_{oo} at node-10 to 36
	0°	10°	20°	30°	40°	50°	60°	70°	80°	90 to 360°
0.00071	1678.83	1764.26	1796.22	1813.63	1824.79	1832.65	1838.53	1843.12	1846.81	1849.87
0.00072	1610.88	1695.90	1727.79	1745.18	1756.34	1764.20	1770.07	1774.66	1778.36	1781.42
0.00073	1546.59	1631.21	1663.04	1680.40	1691.55	1699.41	1705.28	1709.87	1713.57	1716.63
0.00074	1485.74	1569.95	1601.70	1619.05	1630.19	1638.04	1643.92	1648.51	1652.21	1655.27
0.00075	1428.08	1511.89	1543.57	1560.89	1572.03	1579.87	1585.75	1590.34	1594.04	1597.11
0.00076	1373.42	1456.82	1488.42	1505.72	1516.85	1524.70	1530.57	1535.16	1538.86	1541.93
0.00077	1321.57	1404.54	1436.08	1453.35	1464.47	1472.32	1478.19	1482.78	1486.49	1489.55
0.00078	1272.33	1354.89	1386.35	1403.61	1414.72	1422.56	1428.43	1433.02	1436.73	1439.80
0.00079	1225.56	1307.70	1339.08	1356.31	1367.42	1375.25	1381.13	1385.72	1389.42	1392.50
0.0008	1181.10	1262.81	1294.12	1311.33	1322.42	1330.25	1336.13	1340.72	1344.43	1347.50
0.00081	1138.81	1220.09	1251.33	1268.51	1279.59	1287.42	1293.29	1297.88	1301.59	1304.67
0.00082	1098.56	1179.41	1210.56	1227.72	1238.79	1246.62	1252.49	1257.08	1260.79	1263.87
0.00083	1060.22	1140.64	1171.71	1188.84	1199.91	1207.73	1213.60	1218.19	1221.91	1224.98
0.00084	1023.69	1103.67	1134.66	1151.77	1162.82	1170.64	1176.51	1181.11	1184.82	1187.90
0.00085	988.85	1068.39	1099.31	1116.39	1127.43	1135.25	1141.12	1145.71	1149.43	1152.50
0.00086	955.62	1034.72	1065.55	1082.61	1093.64	1101.45	1107.32	1111.92	1115.63	1118.71

Table-3 : Temperatures (°C) attained in different depths at various nodes in 6.6 mm diameter rod

Final Temperatures (°C) attained										
Radial Distance (r) (in mm)	T_n at node-I	T_o at node-2	T_o at node-3	T_u at node-4	T_s at node-5	T_s at node-6	T_n at node-7	T_s at node-8	T_n at node-9	T_{no} to T_{os} at node-10 to 36
	0°	10°	20°	30°	40°	50°	60°	70°	80°	90 to 360°
0.00077	1580.88	1658.57	1687.39	1702.97	1712.90	1719.84	1725.00	1729.01	1732.23	1734.88
0.00078	1521.80	1599.17	1627.93	1643.49	1653.41	1660.36	1665.52	1669.53	1672.75	1675.40
0.00079	1465.68	1542.71	1571.42	1586.97	1596.88	1603.82	1608.98	1613.00	1616.22	1618.87
0.0008	1412.32	1489.03	1517.68	1533.21	1543.12	1550.06	1555.22	1559.23	1562.45	1565.11
0.00081	1361.57	1437.94	1466.53	1482.05	1491.95	1498.89	1504.05	1508.06	1511.29	1513.94
0.00082	1313.27	1389.30	1417.83	1433.33	1443.23	1450.16	1455.32	1459.34	1462.56	1465.22
0.00083	1267.26	1342.95	1371.43	1386.91	1396.80	1403.73	1408.89	1412.91	1416.13	1418.79
0.00084	1223.42	1298.77	1327.18	1342.64	1352.53	1359.46	1364.62	1368.64	1371.87	1374.53
0.00085	1181.62	1256.62	1284.98	1300.42	1310.30	1317.23	1322.39	1326.41	1329.63	1332.30
0.00086	1141.74	1216.40	1244.69	1260.11	1269.99	1276.91	1282.08	1286.09	1289.32	1291.99
0.00087	1103.67	1177.98	1206.21	1221.62	1231.48	1238.41	1243.57	1247.59	1250.82	1253.48
0.00088	1067.32	1141.27	1169.44	1184.831	194.68	1201.61	1206.77	1210.79	1214.02	1216.69
0.00089	1032.58	1106.17	1134.28	1149.65	1159.50	1166.42	1171.58	1175.60	1178.83	1181.50
0.0009	999.36	1072.60	1100.65	1115.99	1125.84	1132.76	1137.92	1141.94	1145.17	1147.84
0.00091	967.59	1040.48	1068.46	1083.78	1093.62	1100.54	1105.70	1109.72	1112.95	1115.62
0.00092	937.19	1009.71	1037.63	1052.93	1062.76	1069.68	1074.84	1078.86	1082.09	1084.77

mm diameter of rod. The results of this analysis are shown in **Table-2, 3 & 4** respectively. It is considered that the points at which the material has reached a temperature of 1475°C has got melted and the weld penetration depth is measured from this point to the circumference of the rod.

Experimental Work:

P91 rods of three different diameters (5.5 mm, 6.6 mm & 8 mm), same as those considered for modeling were chosen for the experimental work. Each rod was machined, cleaned with acetone and dried in oven at around 110 degree C. A punch mark was made on the rod to indicate the starting point of the weld. A weld bead was deposited using Nd-YAG type, pulsed mode laser beam welding process as per the standard procedure. The parameters as explained in the section 2.2 were set. Welding was done with commercial grade argon gas flow at 20 LPM in trailing mode with 45 degree nozzle angle. Argon was used for both as shielding and as well as for plasma suppression. After the welding was done, the sample was cut at the center of the weld width using wire cut machine. The cut surface was polished and etched with Vilella's reagent. The sample was examined under the microscope and depth of penetration was measured through out the weld line. The etched samples were viewed in Nikon (Japan) make, SMZ1000 model stereozoom optical microscope having DP70 camera and macrographs of the rods after laser melting of the surface were recorded.

3.0 RESULTS & DISCUSSIONS

Distance from the surface to the fusion boundary was measured from the cross section of the rod after melting it with the laser beam welding machine as described above. **Fig. 4** shows the cross section of the 6.6 mm diameter rod after laser melting with fusion boundary marked on this. The depth of fusion at every node assuming 1475°C as the temperature at which melting begins for this steel was also estimated. Table-5 shows the depths of fusion measured from the rods and those predicted using equation (1) for various nodes in different diameter rods melted using welding parameters given in **Table 1.**

Table-4 : Temperatures (°C) attained in different depths at various nodes in 8 mm diameter rod

Final Temperatures (°C) attained										
Radial Distance (r) (in mm)	T_{n1} at node-1	T_{n2} at node-2	T_{n3} at node-3	T_{n4} at node-4	T_{n5} at node-5	T_{n6} at node-6	T_{n7} at node-7	T_{n8} at node-8	T_{n9} at node-9	T_{n10} to T_{n36} at node-10 to 36
	0°	10°	20°	30°	40°	50°	60°	70°	80°	90 to 360°
0.00077	1912.03	1983.95	2009.98	2023.85	2032.58	2038.63	2043.09	2046.52	2049.26	2051.50
0.00078	1840.38	1912.05	1938.04	1951.90	1960.63	1966.68	1971.13	1974.57	1977.31	1979.55
0.00079	1772.31	1843.73	1869.68	1883.52	1892.25	1898.30	1902.76	1906.19	1908.93	1911.18
0.0008	1707.60	1778.76	1804.67	1818.51	1827.23	1833.28	1837.74	1841.18	1843.92	1846.17
0.00081	1646.05	1716.95	1742.82	1756.65	1765.37	1771.41	1775.87	1779.31	1782.06	1784.31
0.00082	1587.46	1658.11	1683.94	1697.75	1706.47	1712.51	1716.97	1720.41	1723.16	1725.41
0.00083	1531.66	1602.05	1627.84	1641.64	1650.35	1656.40	1660.86	1664.30	1667.04	1669.30
0.00084	1478.49	1548.62	1574.36	1588.15	1596.86	1602.90	1607.36	1610.80	1613.55	1615.81
0.00085	1427.79	1497.66	1523.35	1537.13	1545.83	1551.88	1556.34	1559.78	1562.53	1564.79
0.00086	1379.43	1449.02	1474.67	1488.44	1497.14	1503.18	1507.64	1511.09	1513.84	1516.09
0.00087	1333.26	1402.58	1428.19	1441.94	1450.64	1456.68	1461.14	1464.59	1467.34	1469.60
0.00088	1289.16	1358.22	1383.78	1397.52	1406.21	1412.25	1416.71	1420.16	1422.9	11425.17
0.00089	1247.03	1315.81	1341.32	1355.05	1363.74	1369.78	1374.24	1377.69	1380.44	1382.70
0.0009	1206.74	1275.251	300.72	1314.43	1323.12	1329.16	1333.62	1337.07	1339.82	1342.08
0.00091	1168.21	1236.44	1261.86	1275.56	1284.24	1290.28	1294.75	1298.19	1300.95	1303.21
0.00092	1131.34	1199.29	1224.66	1238.35	1247.02	1253.06	1257.53	1260.98	1263.73	1266.00

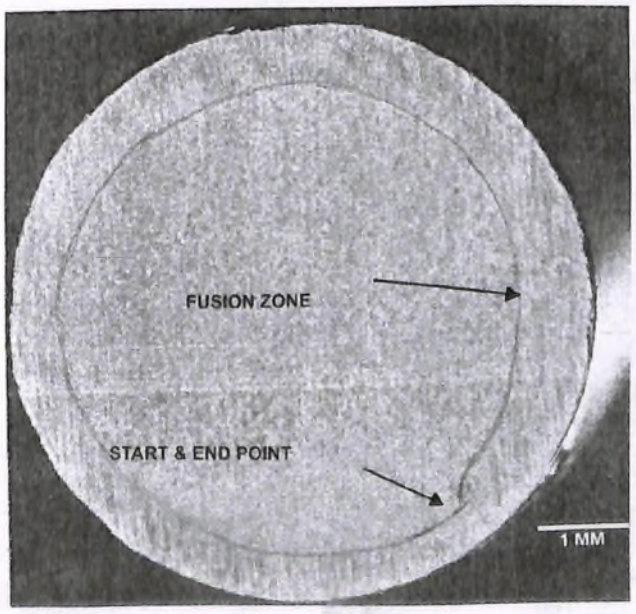

Figure-4: Macrograph of 6.6 mm diameter sample

As we can see from the table that in all the samples, at the nodes between 0° and 30°, the measured depth of fusion is less by 20 to 50 microns when compared to the calculated depth of fusion. However at nodes between 30° and 180° the measured depth of fusion is comparable and matches with the calculated depth of fusion. Similarly when we analyze the depth of fusion at nodes between 180° and 360° it can be seen that the measured values are more by 20 to 120 microns when compared to that of predicted. This can be explained by the fact that the analytical calculation has been done assuming the work piece as an infinite body whereas, the actual sample that was welded is a finite body with circular cross section. Further, latent heats of fusion and transformation have not been considered in this analytical calculation. These could contribute to observed differences in the depths of fusion actually measured and those predicted. Results obtained from this study can be used to estimate the extent of ramping to be done during the second half of the welding so that the depth of fusion is maintained constant throughout the circumference of

Table-5 : Depth of penetration at various nodes in different diameter of rods

Diameter of rods		Depth of penetration (in mm)					
		0°	30°	90°	180°	270°	360°
5.5 mm	Calculated	0.74	0.76	0.77	0.77	0.77	0.77
	Measured	0.71	0.78	0.79	0.80	0.86	0.90
6.6 mm	Calculated	0.78	0.81	0.815	0.82	0.82	0.82
	Measured	0.732	0.833	0.866	0.880	0.891	0.921
8.0 mm	Calculated	0.84	0.86	0.87	0.87	0.87	0.87
	Measured	0.791	0.831	0.860	0.882	0.92	1.0

the rod. This information could in turn be useful in choosing the welding parameters for end plug welding of ferritic steel clad tubes.

It can also be seen from the data that the depth of fusion at various nodes increases as the diameter of the rod increases. This is due to increase in the total heat input as the diameter of rod increases.

As the diameters of the rods taken in this analysis work are small, only 36 numbers of nodes have been taken and the analysis could be done in Microsoft Excel. In case of analysis of weld on larger diameter of rods we may have to take more number of nodes for more accurate results and to get smooth profiles. The results will be more accurate if the size of the job is larger, since the assumption of infinite will be better matched.

Due to various assumptions and approximations made on properties of the material, dimensions of the components and number of nodes taken for calculations, there are variations of up to 30 microns at the beginning of the fusion zone and up to 200 microns at the end of the fusion zone for the predicted fusion depth from the measured depth. These are depicted pictorially in **Figures 5-7**.

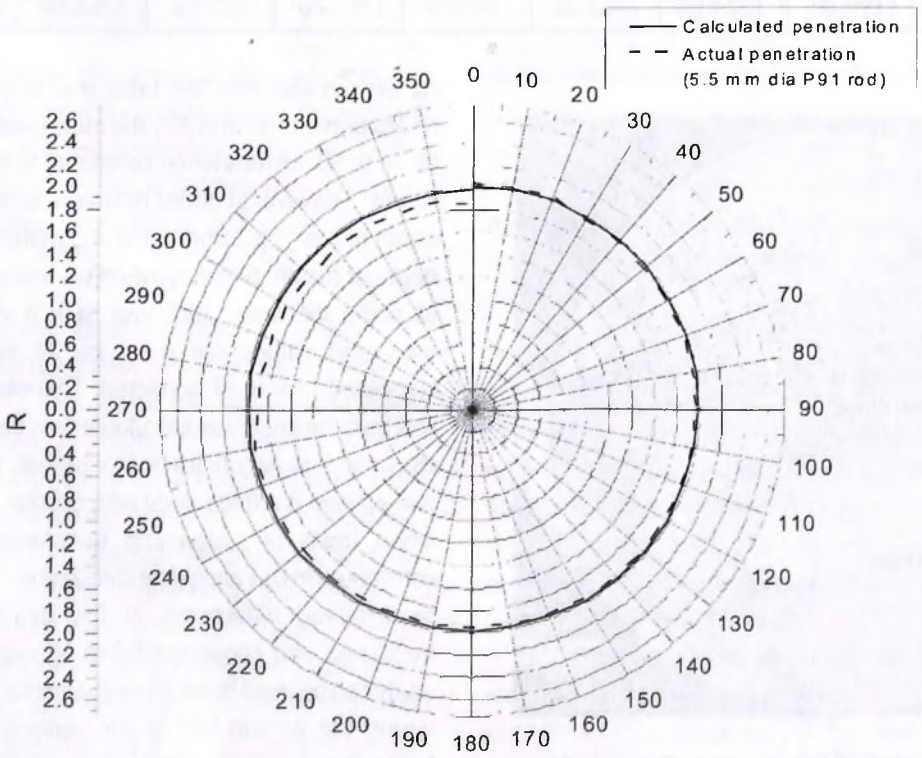

Fig. 5 : Depth of penetration plotted in Origin for 5.5 mm rod sample

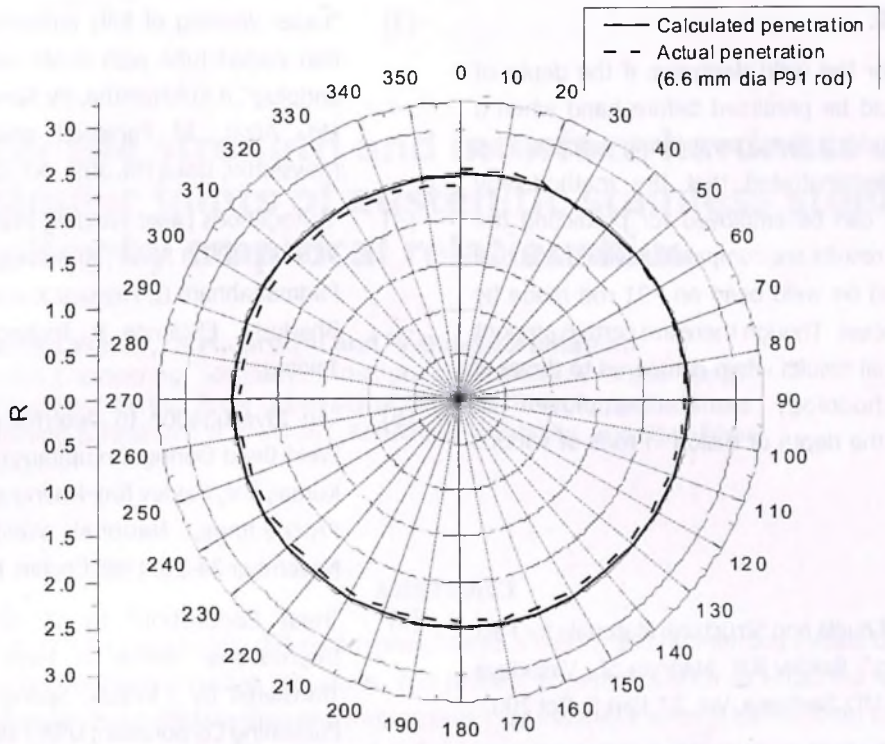

Fig. 6 : Depth of penetration plotted in Origin for 6.6 mm rod sample

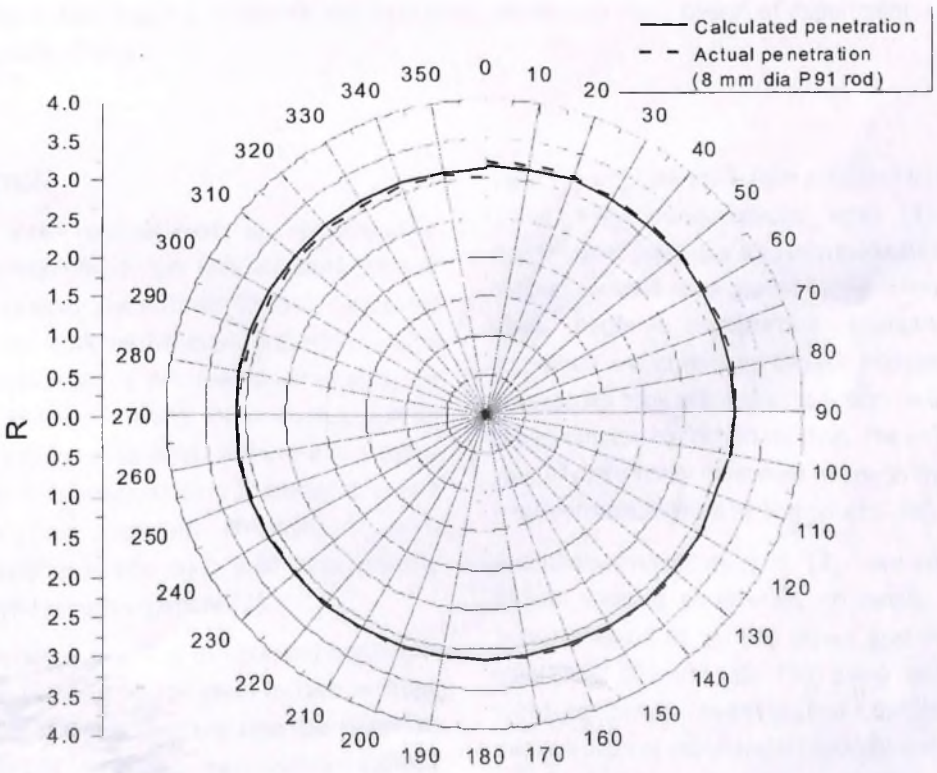

Fig. 7 : Depth of penetration plotted in Origin for 8 mm rod sample

4.0 CONCLUSIONS:

It will be very useful for the weld designers if the depth of fusion/ penetration could be predicted before hand when a welding is carried out under a particular welding process. This analytical work has demonstrated that the methodology presented in this work can be employed for predicting the depth of fusion and the results are comparable with the actual depth of fusion obtained on weld bead on P91 rod made by Laser Beam Welding process. Though there are certain amount of deviations in the actual results when compared to those of calculated, the methodology can be employed to approximately find out the depth of fusion in rods of various diameters.

5.0 REFERENCES:

[1] "Development of Fuels and Structural Materials for Fast Breeder Reactors", Baldev Raj, Mannan SL, Vasudeva Rao PR, Mathew MD, Sadhana, Vol. 27, Part 5, Oct 2002

[2] "Experimental Study on welding of modified 9Cr-1Mo (T91) clad tube to end plug for fabrication of test fuel pins", Prabhu TV, Padmanaban R, Ravishankar G, Srinivasan G, Shaju K Albert, Bhaduri AK, National Welding Seminar, 2009, Kokatta

[3] "Laser Welding of fully austenitic stainless steel (D9) thin walled tube with 316M austenitic stainless steel endplug", A Kulshrestha, PV Suresh, A Gupta, RB Bhutt, Md. Afzal, JP Panakkal and HS Kamath, BARC Newsletter, Issue No. 309, Oct 2009

[4] "Autogenous Laser Welding Investigations on Modified 9Cr-1Mo (P91) Steel", Shanmugarajan Balasubramani, Padmanabham G, Hemant Kumar, S.K. Albert and A.K. Bhaduria, EScience & Technology of Welding and Joining

[5] "An Investigation to Determine the Depth of GTAW Weld Bead During Circumferential Welding on a Rod", Kumar, P.V., Baldev Raj, Rodriguez, P. and Achar, D.R.G. Proceedings, National Welding Seminar 1988, November 24-26, 1988 Cochin, R4.1-R4.6

[6] "Heat Conduction" by U. Grigull & H. Sandner; International Series in Heat and Mass Transfer; Translated by J Kristin; Springer-Verlag; Hemisphere Publishing Corporation; USA 1984

[7] "Properties of materials for the design of Prototype Fast Breeder Reactor Components", a design note no. PFBR/01000/DN/1000/R-E